JVI Journals.ASM.org

Receptor Variation and Susceptibility to Middle East Respiratory Syndrome Coronavirus Infection

Arlene Barlan,[a] Jincun Zhao,[b] Mayukh K. Sarkar,[a] Kun Li,[c] Paul B. McCray, Jr.,[c] Stanley Perlman,[b] Tom Gallagher[a]

Department of Microbiology and Immunology, Loyola University Medical Center, Maywood, Illinois, USA[a]; Department of Microbiology[b] and Department of Pediatrics,[c] University of Iowa, Iowa City, Iowa, USA

ABSTRACT

The Middle East respiratory syndrome coronavirus (MERS-CoV) recently spread from an animal reservoir to infect humans, causing sporadic severe and frequently fatal respiratory disease. Appropriate public health and control measures will require discovery of the zoonotic MERS coronavirus reservoirs. The relevant animal hosts are liable to be those that offer optimal MERS virus cell entry. Cell entry begins with virus spike (S) protein binding to DPP4 receptors. We constructed chimeric DPP4 receptors that have the virus-binding domains of indigenous Middle Eastern animals and assessed the activities of these receptors in supporting S protein binding and virus entry. Human, camel, and horse receptors were potent and nearly equally effective MERS virus receptors, while goat and bat receptors were considerably less effective. These patterns reflected S protein affinities for the receptors. However, even the low-affinity receptors could hypersensitize cells to infection when an S-cleaving protease(s) was present, indicating that affinity thresholds for virus entry must be considered in the context of host-cell proteolytic environments. These findings suggest that virus receptors and S protein-cleaving proteases combine in a variety of animals to offer efficient virus entry and that several Middle Eastern animals are potential reservoirs for transmitting MERS-CoV to humans.

IMPORTANCE

MERS is a frequently fatal disease that is caused by a zoonotic CoV. The animals transmitting MERS-CoV to humans are not yet known. Infection by MERS-CoV requires receptors and proteases on host cells. We compared the receptors of humans and Middle Eastern animals and found that human, camel, and horse receptors sensitized cells to MERS-CoV infection more robustly than goat and bat receptors. Infection susceptibility correlated with affinities of the receptors for viral spike proteins. We also found that the presence of a cell surface lung protease greatly increases susceptibility to MERS-CoV, particularly in conjunction with low-affinity receptors. This cataloguing of human and animal host cell factors allows one to make inferences on the distribution of MERS-CoV in nature.

The Middle East respiratory syndrome coronavirus (MERS-CoV) emerged into the human (Hu) population in April 2012 (1). This enveloped RNA virus is acquired by respiratory spread, either from infected humans or from nonhuman animals. In individuals with underlying comorbidities such as diabetes or respiratory or renal disease, infection by this virus can cause widespread pneumonia (2, 3), with case fatality rates of ~40% (4, 5). While possible treatment options for this devastating infection may be forthcoming (6, 7), longer-term approaches to limiting human MERS-CoV infections will come after identifying and quarantining the animal source(s) of this virus.

Bats (Bt) are implicated as virus reservoirs, as several known bat CoV genomes closely match MERS-CoV (8–10), and bats harbor the progenitors to human severe acute respiratory syndrome (SARS)-CoV (11). Camels are also suspected virus reservoirs, because MERS-CoV-neutralizing antibodies are prevalent in camel herds from neighboring countries as well as Egypt and the Canary Islands (12, 13). Further, MERS-CoV RNA was detected in a camel herd in Qatar, and two individuals who became infected with the virus were in contact with these animals (14). Notably, there may be several animal reservoirs, as phylogenetic analyses suggest that there have been multiple, geographically distinct MERS-CoV transmissions from animals to humans (15). Indeed, given that current human-to-human transmissibility indices are low (16) and that animals might asymptomatically and abundantly shed virus, the animal-to-human transmission route may well account for the majority of MERS-CoV-infected patients.

While widespread sampling of Saudi Arabian animals will help to identify sources of the virus, a complementary strategy is to carefully assess the infection sensitivities of cells from different animal species. Several laboratories have identified MERS-CoV-susceptible cell types, which include human, bat, rabbit, and pig (17). Thus, these animals express MERS-CoV susceptibility factors, including the MERS-CoV receptor dipeptidyl peptidase 4 (DPP4; also known as CD26) (17) and quite likely the proteases that cleave the MERS-CoV S proteins and allow them to refold into membrane fusion-active forms (18, 19). The widespread and relatively conserved nature of these susceptibility factors likely accounts for the remarkable polytropic character of MERS-CoV.

What are not known, however, are the relative extents to which the DPP4s of each animal sensitize cells to MERS-CoV infection. Organizing animal DPP4s according to their affinity for MERS-

Received 17 January 2014 **Accepted** 11 February 2014
Published ahead of print 19 February 2014
Editor: T. S. Dermody
Address correspondence to Tom Gallagher, tgallag@lumc.edu.

doi:10.1128/JVI.00161-14

CoV, and according to their effectiveness at supporting virus entry, will add to our understanding of animal reservoirs and virus transmission pathways. Furthermore, comparative analyses of animal DPP4s and associated host proteases will address important questions concerning MERS-CoV adaptation to a narrower range of species, including humans. Our results reveal a hierarchy in animal DPP4 abilities to sensitize cells to MERS-CoV infection and also demonstrate that the presence of a relevant host protease can potentially alter this hierarchy.

MATERIALS AND METHODS

Cells. 293β5, 293T, and 293EBNA cells and Vero E6 cells were maintained in DMEM-10 (Dulbecco modified Eagle medium [DMEM] supplemented with 10% heat-inactivated fetal bovine serum [FBS; Atlanta Biologicals], 100 IU/ml penicillin, 1 mg/ml streptomycin, 0.1 mM nonessential amino acids, 1 mM sodium pyruvate, 10 mM HEPES, and 2 mM L-glutamine [HyClone]). 293β5 and 293T cells were obtained from Christopher Wiethoff and Edward Campbell at Loyola University Medical Center (LUMC). Mouse (Ms) astrocytoma DBT cells were maintained in MEM-7.5 (minimal essential medium [MEM] supplemented with 7.5% FBS, 10% tryptose phosphate broth [Difco], 100 IU/ml penicillin, 1 mg/ml streptomycin, and 2 mM L-glutamine). All cell lines were propagated as adherent monolayer cultures.

Plasmids and construction of chimeric receptors. Untagged mouse (Ms) DPP4 plasmid pCMV-Kan/Neo-msDPP4 (GenBank BC022183) and C-terminal Myc/FLAG-tagged human (Hu) DPP4 plasmid pCMV6-Entry-huDPP4 (NCBI Reference Sequence NM_001935) were purchased from OriGene. pCMV-Kan/Neo-msDPP4 was PCR amplified with the following primers: AsiSI-forward (5′-TTGGCGATCGCCATGAAGACA CCGTGGAAG-3′) and NotI-reverse (5′-ATAGTTTAGCGGCCGCAGT GTAAGGAGAAGCACTGCT-3′). Subsequently, MsDPP4 was cloned into pCMV6-Entry vector between 5′ AsiSI and 3′ NotI sites. The MsDPP4 vector was then PCR amplified with the following primers: forward, 5′-A GTACCACGGGCTGG-3′; reverse, 5′-CTCTTCATAAACCCAGTC-3′. Synthetic DNAs encoding DPP4 blades 4 and 5 [(b4–5)] of human (Hu), horse (Hs; NCBI Reference Sequence accession no. NC_009161.2), Dubai camel (Cm), goat (Gt; GenBank accession no. AJPT00000000), and pipistrelle bat (Bt; GenBank accession no. KC249974.1) were purchased from GenScript. The camel sequence was obtained by reverse transcription-PCR (RT-PCR) and sequencing from a *Camelus dromedarius* cell line (Dubca; ATCC CRL 2276). Gibson assembly techniques (20) and an In-Fusion HD cloning system (Clontech) were then used to insert the various sets of animal DPP4 blades 4 and 5 (b4–5) into the MsDPP4 vector. The chimeric DPP4 receptors were designated human [Hu(b4–5)], horse [Hs(b4–5)], camel [Cm(b4–5)], goat [Gt(b4–5)], and bat [Bt(b4–5)]. pCAGGS-TMPRSS2-FLAG and pCAGGS-TMPRSS2(S441A)-FLAG were previously constructed (21). Codon-optimized MERS S containing a C9 tag was purchased from Genscript and subsequently cloned into pcDNA3.1+ between the EcoRI and NotI restriction sites.

Transfections. Transfections were performed with polyethylenimine (PEI; Polysciences) at a ratio of 1 μg DNA:3 μg PEI. DNA/PEI complexes were incubated in Opti-MEM (Life Technologies) for 15 min before they were added to plated cells in 6-well or 12-well test plates. One day posttransfection, cells were washed with 0.9% saline solution, treated with trypsin (HyClone), and then replated into 96-well test plates for later inoculation with pseudoviruses or authentic MERS-CoV.

Pseudovirus production and transduction assays. To generate vesicular stomatitis virus luciferase (VSVluc)-MERS S pseudovirus, 293T cells were transfected with pcDNA3.1-MERS-S-C9 via PEI transfection. One day posttransfection, cells were inoculated with G*ΔG-VSV-luc per the recommendations in reference 22. One day later, media were collected, clarified for 10 min at 1,000 × *g*, labeled as VSVluc-MERS S, and stored at −80C. For transduction assays, 293β5 or DBT cells were first transfected via PEI with the various chimeric DPP4 receptor constructs. After 24 h, cells were then transduced with VSVluc-MERS S. At 16 h after pseudovirus transduction, cells were washed with serum-free DMEM (SFM) and then lysed with 1× passive lysis buffer (Promega). Luminescence was measured after addition of luciferase substrate (Promega) using a Veritas microplate luminometer (Turner BioSystems).

MERS-CoV infections. DBT cells were transfected with chimeric DPP4 cDNAs and inoculated 24 h later with MERS-CoV at 1 PFU per cell. After 1 h at 37°C, inocula were removed and cells incubated for 48 h. Supernatants were collected and infectivities determined by plaque assays on Vero 81 cells.

MERS S1-Fc production. The MERS S1 coding sequence (human codon optimized) was PCR amplified with the following primers: NotI-forward (5′-CTAGCGGCCGCAGCCATGATCCATAGCGTCTTCCTC C-3′) and ClaI-reverse (5′-ATCGATATACTTACCTGTGGGGGTCAGA GTGGAGGGGGT-3′). The resulting S1-encoding fragment was then recombined via Gibson assembly techniques with a vector fragment that was PCR amplified from pCEP4-sMHVR-Ig (23) using the following primers: ClaI-forward (5′-ACCCCCTCCACTCTGACCCCCACAGGTA AGTATATCGAT-3′) and NotI-reverse (5′-GGAGGAAGACGCTATGG ATCATGGCTGCGGCCGCTAG-3′).

The resulting plasmid, designated pCEP4-MERS-S1-Fc, was transfected using PEI into 293 EBNA cells, which contain the Epstein-Barr virus (EBV) EBNA-1 protein necessary for stable maintenance of transfected pCEP4 plasmid DNAs. After 36 h, cells were washed with prewarmed SFM and incubated in SFM for ~16 h. Conditioned media were collected, and cells were returned to DMEM-10 for ~8 h and then placed back with SFM for a subsequent round of S1-Fc secretion and collection. Pooled collections of S1-Fc-containing SFM were concentrated ~100-fold using Centricon-30 centrifugation devices (Millipore). Quantifications of MERS S1-Fc protein yields were determined by comparisons with serial dilutions of human IgG standards on Western immunoblots, with band intensities quantified by charge-coupled-device (CCD) Alphaview instrumentation and software (Protein Simple).

MERS S1-Fc blocking assay. DBT cells were transfected with the various chimeric DPP4 receptor constructs in 12-well cell culture plates at a seeding density of 3.8×10^5 cells/well. One day posttransfection, cells were trypsinized and replated in 96-well plates. MERS S1-Fc was added at indicated concentrations and incubated at 37°C for 1 h, followed by addition of VSVluc-MERS S pseudoviruses. At 16 h postransduction, cells were lysed with 1× passive lysis buffer (Promega) and luminescence was measured as described above.

Flow cytometry. DBT cells were transfected with the various chimeric DPP4 receptor constructs, at 1 μg DNA per 10^6 cells. One day later, cells were detached from plates using Accutase (Millipore), suspended, and washed in phosphate-buffered saline (PBS)–2% FBS. Cells were incubated with rabbit anti-FLAG antibody (1:500) (Sigma F7425) or MERS S1-Fc (~50 nM) for 1 h on ice, followed by either Alexa Fluor 488 goat anti-rabbit IgG (Lifetech) (1:1,000) or Dylight549 goat anti-human IgG (Pierce) (1:1,000) for 1 h on ice. Cells were analyzed using an LSR Fortessa (BD Biosciences). Data were analyzed using FlowJo software.

TMPRSS2 titration and transduction. DBT cells were PEI transfected in 12-well test plates with Ms DPP4, Hu(b4–5), or Bt(b4–5) with an increasing level of TMPRSS2 or TMPRSS2(S441A). One day posttransfection, cells were reseeded into 96-well plates. At 6 h later, the cells were transduced with VSVluc-MERS S and luminescence was measured 16 h postransduction as described above.

Cell lysis and Western blot analysis. Transfected cells were dissolved on ice for 15 min with TX100 buffer (1% Triton X-100, 25 mM Tris-HCl [pH 7.4], 125 mM NaCl, 0.1% protease inhibitors, 1 mM $MgCl_2$, 1 mM $CaCl_2$) and nuclei removed by centrifugation. Postnuclear supernatants were mixed 1:5 with SDS buffer (0.375 M Tris HCl [pH 6.8], 10% SDS, 6% 2-mercaptoethanol, 30% glycerol, 0.375 M Tris HCl [pH 6.8]) and heated to 95C for 5 min. A total of 30,000 cell equivalents were subjected to SDS-PAGE and proteins transferred to polyvinylidene difluoride (PVDF) membranes (Millipore). DPP4 and TMPRSS2 proteins were detected with

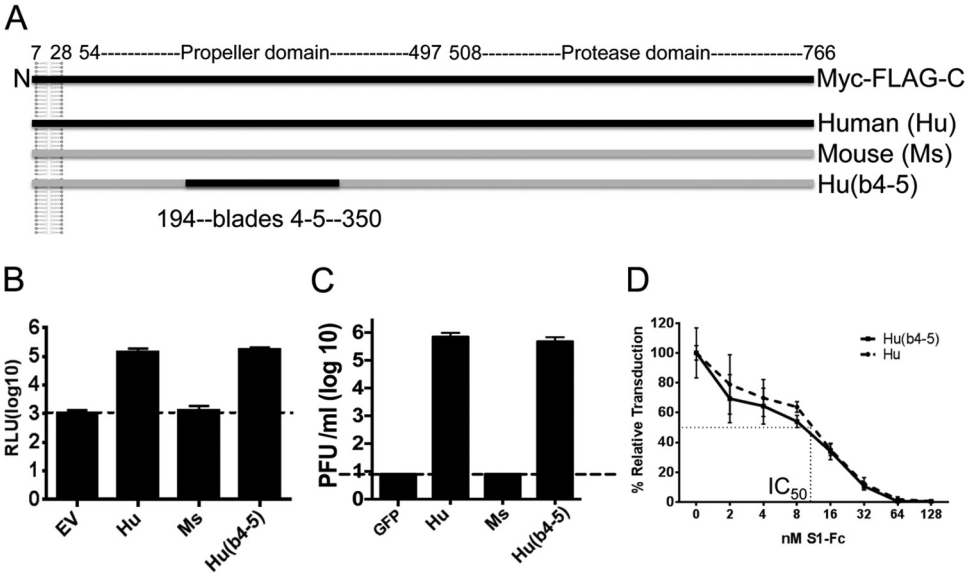

FIG 1 Properties of Hu and Hu(b4–5) DPP4s. (A) DPP4 includes a transmembrane anchor (residues 7 to 28), a propeller ectodomain (54 to 497), and a protease ectodomain (508 to 766). Exchangeable blades 4 and 5 comprise residues 194 to 350. Hu and Ms DPP4s are in black and gray, respectively. (B) Mouse DBT cells were transfected with pcDNA3.1 (empty vector [EV]) Hu, Ms, or Hu(b4–5) DPP4s and then transduced 1 day later with VSVluc-MERS S. At 16 h postransduction, relative luminescence unit (RLU) values were measured and plotted. (C) Mouse DBT cells were transfected and infected 1 day later with MERS-CoV (multiplicity of infection [MOI] = 1). Secreted viruses were collected after 2 days, and infectivities (PFU/ml) were determined by titration on Vero cell indicators. The hatched horizontal line indicates the lower limit of assay sensitivity. GFP, green fluorescent protein. (D) Mouse DBT cells were transfected and, after 1 day, exposed to the indicated doses of MERS S1-Fc. After 1 h at 37°C, VSVluc-MERS S was inoculated, with MERS S1-Fc concentrations remaining the same. At 16 h postransduction, luminescence values were measured and the relative transduction values were quantified. The concentration of MERS S1-Fc at the IC_{50} reflects the affinity of MERS S for the DPP4 receptors. In all data sets, the error bars indicate the standard errors of the means from triplicate values. Each experiment was repeated twice.

rabbit anti-FLAG (Sigma F7425) (1:1,000) and peroxidase-conjugated goat anti-rabbit IgG (Pierce) (1:5,000). Actin was detected with anti-β-actin peroxidase (Sigma) (1:20,000). Membranes treated with ECL substrate (Pierce) were detected with FluorChem E and analyzed with Alphaview software (Protein Simple).

Statistical analyses. Statistical tests of significance were performed using the Holm-Sidak multiple Student's *t* test procedure.

Nucleotide sequence accession number. The complete camel DPP4 open reading frame was deposited in NCBI GenBank (accession number KJ002534).

RESULTS

Chimeric human-mouse DPP4 receptors. CD26/DPP4 is a type II integral membrane protein, organized as a homodimer, with each monomer comprising a membrane-proximal α/β hydrolase domain and a membrane-distal β-propeller domain (24) (Fig. 1A). The receptor-binding domains (RBDs) of the MERS-CoV S proteins (25) bind to human blades 4 and 5 of the 8-blade β-propeller (26, 27). Human blades 4 and 5 also bind extracellular adenosine deaminase (ADA) (28), tethering this enzyme to $DPP4^+$ T cells to provide local control of adenosine levels (29). Murine DPP4, however, does not bind ADA (28), and murine DPP4 is indeed divergent from human DPP4 in the blade 4 and 5 region. This divergence suggests that murine DPP4 cannot bind MERS-CoV S proteins and provides an explanation for the observation that MERS-CoV does not infect murine cells (17) or mice (30, 31).

However, murine and human DPP4s are conserved at the flanking blade 3 and 6 regions. Therefore, we reasoned that murine blades 4 and 5 could be replaced with orthologous animal blades, without perturbing the seams between the murine and animal blades. We expected that, unlike the parental murine DPP4, some chimeric DPP4s would function as MERS-CoV receptors, with the receptor functions reflecting the complete native animal DPP4s. This expectation was based on the fact that the close contacts between MERS-CoV S and human DPP4 are within the blade 4 and 5 region (17, 27).

We obtained cDNA clones encoding C-terminal myc and FLAG-tagged mouse (Ms) and human (Hu) DPP4s and synthetic DNAs encoding Ms and Hu blades 4 and 5. Gibson assembly techniques (20) were then used to replace the Ms blades with the synthetic human DNA and to reciprocally replace Hu with Ms blades. This provided the construct designated Hu(b4–5), with humanized amino acids 194 to 350 in the Ms DPP4 background (Fig. 1A). The parental and chimeric DPP4s were evaluated by assessing their abilities to sensitize mouse DBT cells to MERS-CoV. Mouse DBT cells were chosen for these experiments because, unlike many human cell lines, they were completely refractory to MERS-CoV infection and thus might be rendered susceptible by receptor expression. In a first test, we challenged DPP4-transfected DBT cells with VSV pseudoparticles (22) that encode firefly luciferase (luc) and also display MERS S on their surfaces (VSVluc-MERS S). These pseudoviruses serve as surrogates of authentic MERS-CoV, with fluorescent luc (Fluc) activities after transduction being readouts of potential cell susceptibility to infection. By these assays, Hu DPP4 and the chimeric Hu(b4–5) equally sensitized cells to transduction whereas the Ms DPP4 did not (Fig. 1B). Notably, the reciprocal chimeric Hu DPP4 with Ms blades 4 and 5 also did not sensitize cells to transduction (data not shown). In a second test, we challenged the DBT cell transfectants with authentic MERS-CoV and measured virus

output titers by plaque assays. The HuDPP4 and Hu (b4–5) DPP4-positive (DPP4$^+$) cells supported MERS-CoV infection equally well (Fig. 1C). Thus, in these assays, the readouts from VSVluc-MERS S pseudovirus transductions paralleled the readouts from authentic MERS-CoV infections. Additionally, the human DPP4 was indistinguishable from a mouse DPP4 that contained only human blades 4 and 5.

To further compare Hu DPP4 with the Hu(b4–5) DPP4, we measured affinities of these receptors for MERS S proteins. Coronavirus S1-Fc proteins are surrogates for authentic viral S (32), and MERS S1-Fc proteins are known to block both MERS S-mediated transduction and MERS-CoV infection (33). To compare the affinities of the two DPP4s for viruses, we introduced graded doses of MERS S1-Fc proteins before and during VSVluc-MERS S transduction. While control N-carcinoembryonic antigen-related cell adhesion molecule (CEACAM)-Fc proteins (23) had no effect on transduction (data not shown), the S1-Fc proteins blocked transduction into Hu and Hu(b4–5) DPP4-positive cells with equal effectiveness (Fig. 1D). These analyses further demonstrated that the S1-Fc 50% inhibitory concentrations (IC_{50}) were ~10 nM for both receptors. These ~10 nM affinity measurements were similar to the recently reported Biacore determination of 17.6 nM affinity between human DPP4 and S1 (26).

Chimeric animal DPP4 receptors. These results from comparisons of Hu and Hu(b4–5) DPP4s engendered confidence that the animal blade 4 and 5 regions, placed in the Ms DPP4 context, would reflect the complete animal DPP4s, at least with respect to MERS-CoV entry. Therefore, we proceeded with additional blade 4 and 5 replacements from other animals. For this study, we focused on DPP4s from indigenous Middle East animals that are considered to be potential carriers of MERS-CoV. This included Dubai camels, from which we obtained the complete DPP4 cDNA sequence by RT-PCR and rapid amplification of cDNA ends (RACE). The camel DPP4 sequence was compared with other animal DPP4 sequences in a phylogenetic analysis (Fig. 2). The comparisons also included Pipistrelle bats, one of ~20 bat genera residing in Saudi Arabia. We note, however, that *Pipistrellus kuhlii* is the native Saudi Arabian species, while *Pipistrellus pipistrellus* is the bat DPP4 that we evaluated.

DPP4 blade 4 and 5 amino acid sequences from these animals diverge increasingly from those from humans in the order shown in Fig. 3: horses, camels, goats, bats, and then mice. With respect to the 14 residues contacting S proteins at <3.6 Å (Fig. 3, arrows; see also reference 27), horses have 0, camels 2, goats and bats 3, and mice 5 residues diverging from those of humans. Of note, K392 in blade 6 is close to MERS-CoV S1 in the cocomplex structure (27). While blades 4 and 5 make the key contacts, it is possible that this residue, which also differs among species, could have an additional small effect on MERS-CoV binding.

All of the chimeric DPP4s sensitized DBT cells to VSVluc-MERS S transduction but at various levels (Fig. 4A). Human, horse, and camel receptors were similarly effective, while goat and bat conferred significantly lower susceptibilities. These trends were also identified in the results of authentic MERS-CoV infections (Fig. 4B). These trends did not arise from relative underexpression of the goat and bat DPP4 chimeras, as assessed by Western immunoblotting (Fig. 4C). Notably, relative to the transduction assay results, the infection assays revealed far more prominent differences in the receptors' abilities to sensitize cells (note that the Fig. 4A and B *y* axis scales are linear and logarithmic, respectively). This may reflect the fact that the transductions are necessarily single-cycle processes, while the 2-day infections involve multiple cycles of virus entry, release, and reentry, with each entry step being influenced by receptor abundance and affinity. Cumulative low-efficiency entry steps multiply to create greater end-stage differences in authentic MERS-CoV yields.

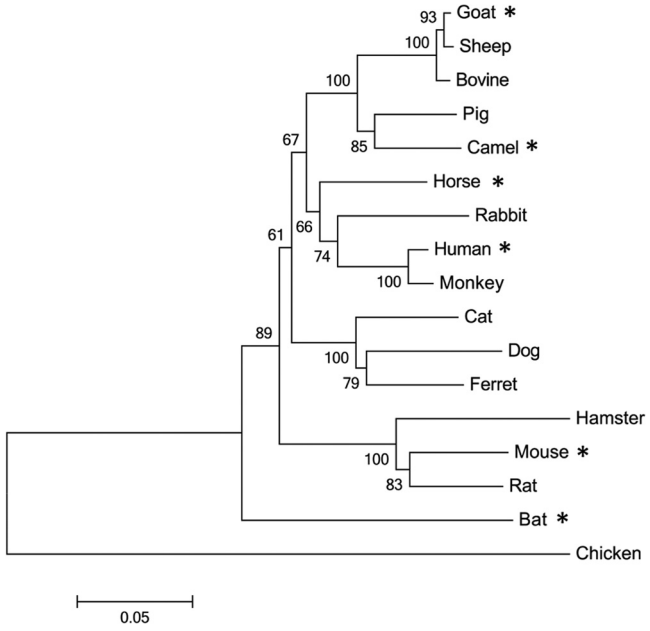

FIG 2 Camel DPP4 sequence and phylogenetic relationships with other animal DPP4s. Camel DPP4 was compared with the indicated animal DPP4 protein sequences using Molecular Evolutionary Genetics Analysis (MEGA; www.megasoftware.net) to generate the neighbor-joined phylogenetic tree. Numbers at each node are bootstrap values calculated from 500 trees and represent the percentages of trees that resolved clades at the indicated endpoints. The scale bar indicates the relationship between line lengths and sequence dissimilarities (0.05 = 5/100 amino acid divergence). Asterisks denote the animal DPP4s evaluated for this report.

S protein affinities for DPP4 receptors. The cell surface receptor level and the receptor affinity for viruses both contribute to sensitize for infection (34). Cell surface receptor levels were assessed by flow cytometry, using antibodies to the extracellular FLAG epitope tags. Consistent with the Western blot analyses (Fig. 4C), the results (Fig. 5) demonstrated that all chimeric receptors were expressed similarly on surfaces, with the minor differences perhaps reflecting slight variations in the ~50%-efficient plasmid DNA transfections. These results indicated that the reduced susceptibilities of goat and bat DPP4$^+$ cells did not result from diminished surface expression but rather from reduced affinities for MERS-CoV. The same DPP4$^+$ transfectants, assessed in parallel for S1-Fc binding, revealed quite similar S1 associations for all of the receptors except for bat and mouse. Notably, the similar S1 associations were observed among fairly divergent receptors.

While flow cytometry results revealed some S-protein affinity differences between the animal DPP4s, they did not provide quantitative binding data, and therefore we adopted the more sensitive approach of measuring affinities via S1-Fc-mediated blockade of MERS S pseudotype transduction. To this end, animal DPP4$^+$ transfectants were incubated with serial dilutions of S1-Fc and then challenged with VSVluc-MERS S. These experiments re-

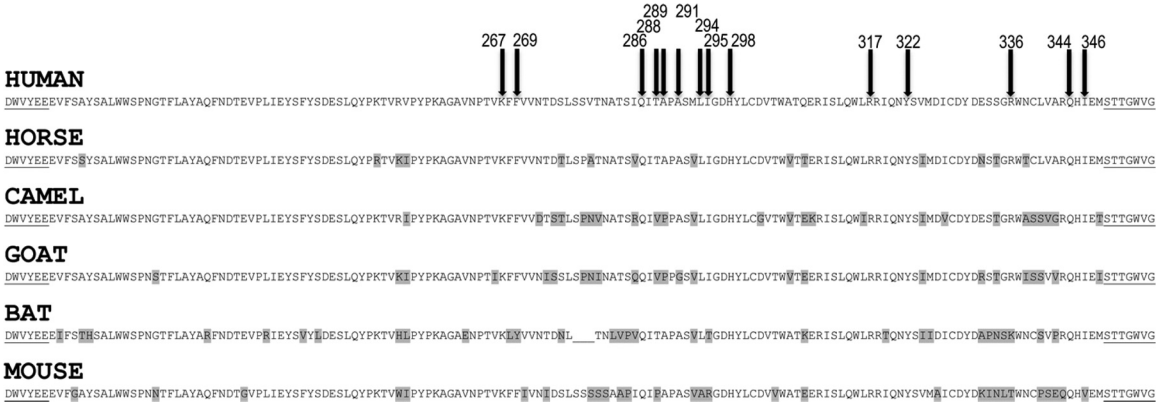

FIG 3 Alignment of DPP4 blade 4 and 5 regions. The human and animal DPP4 sequences are arranged in order of increasing divergence from human blades 4 and 5. Light gray highlighting denotes divergent amino acids. Underlined regions denote the conserved terminal residues comprising the junctions between animal blades 4 and 5 and the mouse DPP4. The arrows and associated numbers at the top point to residues that, in human DPP4, interface closely with the MERS S protein.

vealed that the human DPP4 chimeras had the highest affinities of ~10 nM for S proteins, with the affinities being modestly lower for horse and camel receptors (Fig. 6). In four of four separate experiments, the S1-Fc affinities for Hu(b4–5) exceeded those for Hs(b4–5) and Cm(b4–5) DPP4 chimeras; however, the modest differences between these S1-Fc affinities were not statistically significant. Gt(b4–5), however, had significantly lower affinities of ~40 nM, while Bt(b4–5) receptors bound so weakly with S1-Fc that an accurate affinity determination was not obtained by this method (Fig. 6). These quantitative data concurred with the flow cytometric determinations (Fig. 5) and, in part, with DPP4 phylogenetic relationships (Fig. 2).

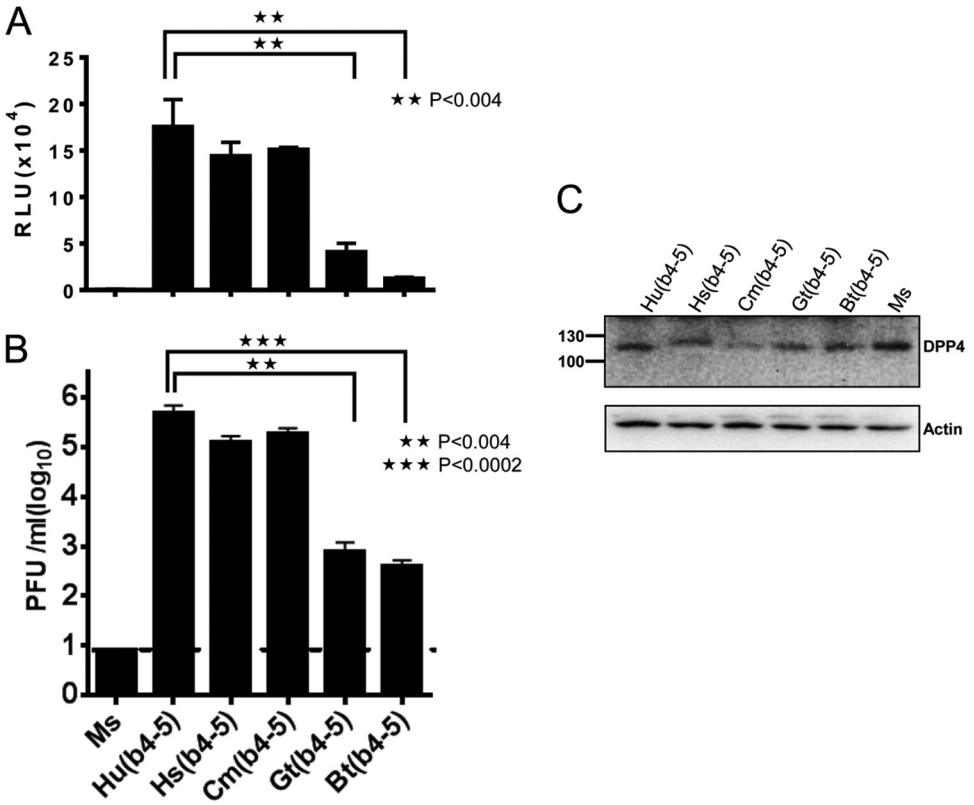

FIG 4 Transduction and infection of animal DPP4-positive cells. (A) DPP4-transfected DBT cells were transfected with the indicated DPP4s and transduced 1 day later with VSVluc-MERS S, and luciferase accumulations were determined 16 h later. Standard errors are shown; $n = 6$. Statistical significance tests were performed using the Student t test. Data shown are representative of five independent results. (B) DBT cells were infected with MERS-CoV, and infectivity in media was quantified by a plaque assay on Vero cells. The hatched horizontal line indicates the lower limit of assay sensitivity. Standard errors are shown; $n = 3$. Statistical significance tests were performed using the Student t test. (C) DPP4-transfected DBT cells were lysed at 1 day posttransfection (the time of pseudovirus and virus inoculation). DPP4 and actin proteins were visualized by immunoblotting.

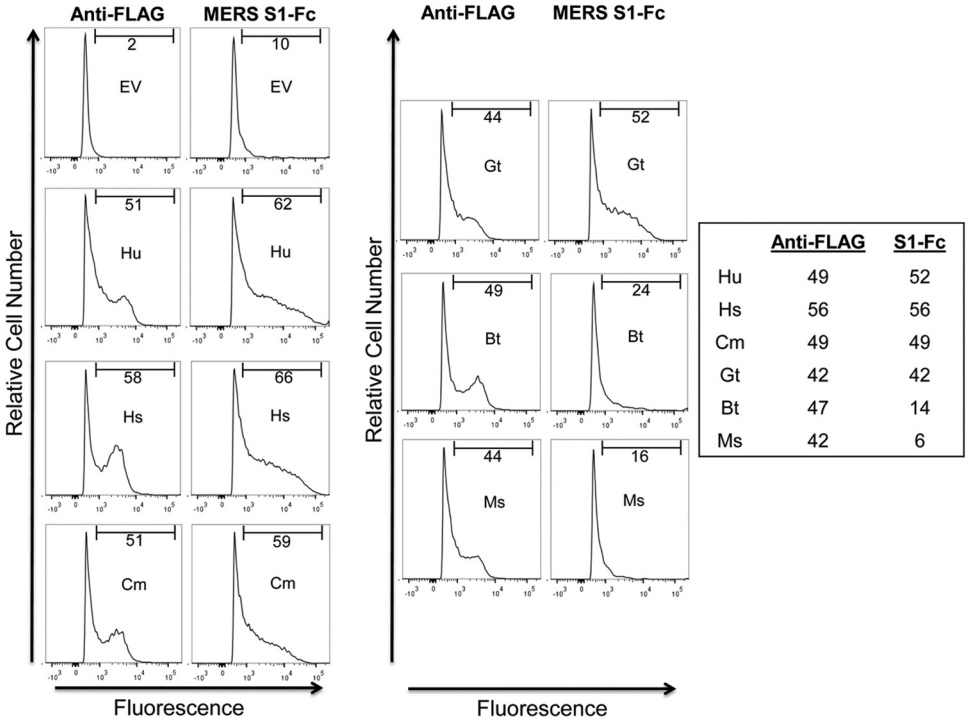

FIG 5 Relative levels of anti-FLAG antibody and MERS S1-Fc binding to cells. DBT cells transfected with pcDNA3.1 (EV), or with pCMV6-DPP4 chimeras, were incubated with anti-FLAG antibodies (1:500), or with 50 nM S1-Fc, for 1 h at 4°C and analyzed by flow cytometry. The bars in each panel indicate positive cell windows, and the numbers under the bars indicate the percentages of anti-FLAG antibody- and MERS S1-Fc-positive cells. Positive cell percentages, after background subtraction, are listed to the right in the figure.

Role of TMPRSS2 proteases. In addition to S-binding receptors, S-cleaving proteases are principal host factors determining the efficiency of CoV entry (35). Indeed, cell surface serine protease TMPRSS2 can augment MERS-CoV infection by up to 100-fold (18, 19). To evaluate the role of TMPRSS2 in relation to DPP4 affinities for MERS-CoV, target cells were transfected with DNAs encoding both DPP4 and TMPRSS2 or with DPP4 and the control, catalytically inactive TMPRSS2 (S441A) (36). The catalytically inactive S441A TMPRSS2 DNA was indistinguishable from empty vector DNA and had no effect on subsequent MERS S-mediated transductions (data not shown). However, relative to the S441A mutant control conditions, TMPRSS2 significantly promoted MERS S-mediated transduction into all of the DPP4$^+$ cells, except those expressing mouse DPP4 (Fig. 7A). We noted a trend in which transduction into cells with relatively low-affinity receptors [Bt(b4–5) and Gt(b4–5)] was augmented by TMPRSS2 more substantially than the corresponding transductions into cells with higher-affinity receptors. Specifically, transduction into Bt(b4–5) and Gt(b4–5) receptor-positive cells was augmented by wild-type (WT) TMPRSS2 ~3.6 times more than the corresponding transduction into Cm(b4–5), Hs(b4–5), and Hu(b4–5) DPP4$^+$ cells. These intriguing findings demanded further investigation by TMPRSS2 titration. In the context of the far less adhesive Bt(b4–5) DPP4, TMPRSS2 stimulated virus entry approximately 10-fold (from ~2-fold to ~20-fold above background levels), while the level of TMPRSS2 stimulation showed a less pronounced ~5-fold increase in the human DPP4 context (Fig. 7B). These were statistically significant differences as assessed by Student's *t* test. Notably, by Western blotting, we detected relatively constant DPP4 levels with increasing TMPRSS2 levels (Fig. 7B, bottom panels). TMPRSS2 was not readily detectable by Western blotting at the plasmid input doses used (data not shown). However, as it is known that the presence of TMPRSS2 results in proteolysis of the

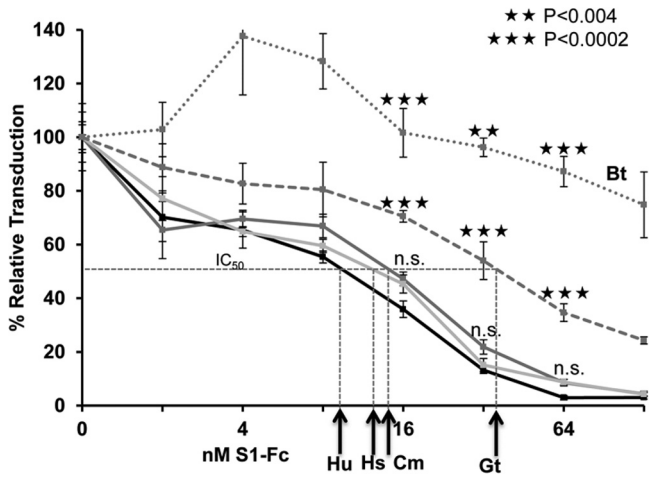

FIG 6 Transduction blockade by MERS S1-Fc. DBT cells were transfected with DPP4 chimeras, incubated with the indicated concentrations of MERS S1-Fc for 1 h at 37°C, and transduced with VSVluc-MERS-S. Luminescence values were measured 16 h later. Data were normalized to transduction in the absence of S1-Fc. The concentrations of S1-Fc at each IC_{50} reflect the affinities of MERS spikes for the different DPP4 receptors. The experiment was repeated four times with similar results. Error bars indicate the standard errors of the means from triplicate values. Student's *t* tests were used to assess the significance of differences between human and animal DPP4 data; n.s. = not significant.

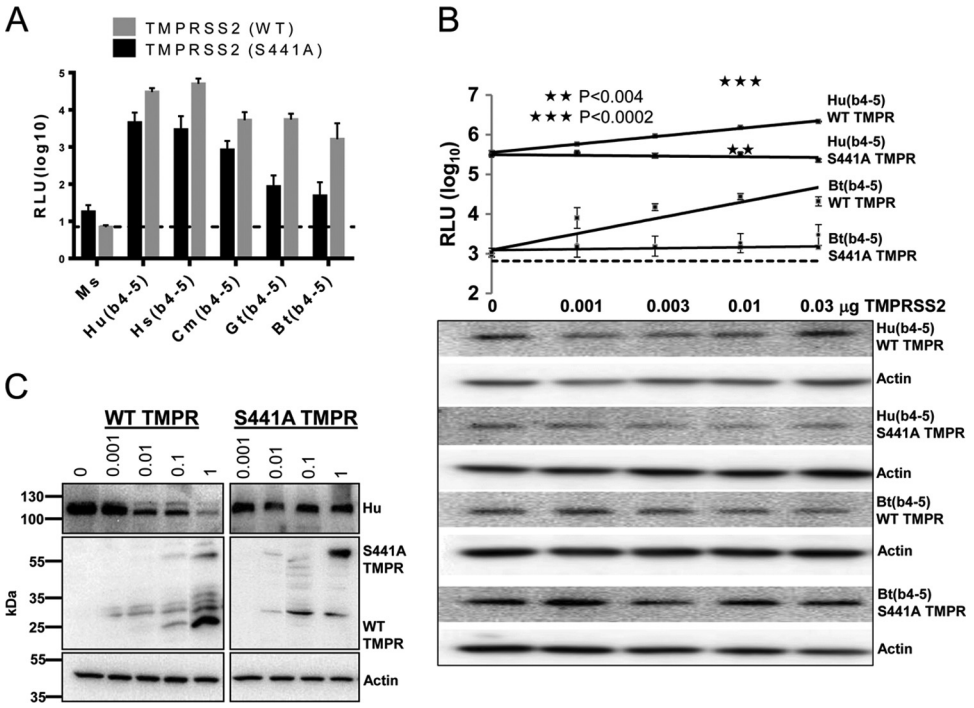

FIG 7 Effect of TMPRSS2 on MERS S-mediated transduction. (A) DBT cells were cotransfected with the indicated DPP4 chimeras and either wild-type (WT) or catalytically inactive (S441A) TMPRSS2 plasmids at 1:0.1 DPP4/TMPRSS2 DNA ratios. After 1 day, cell subsets were transduced with VSVluc-MERS-S, and luciferase values were determined 16 h later. (B) DBT cells were transfected with Hu(b4–5) or Bt(b4–5) DPP4 chimeras, in conjunction with increasing amounts of wild-type (WT) or catalytically inactive (S441A) TMPRSS2 plasmids. After 1 day, cell subsets were transduced with VSVluc-MERS-S, and luciferase values were determined 16 h later. The dotted line designates the basal level of transduction into MsDPP4-transfected cells. Holm-Sidak Student's *t* tests were used to reveal the significance of the relative differences between transduction levels in the presence of S441A and WT TMPRs; *P* values are indicated. To obtain the images beneath the graph, the luciferase-containing lysates were subjected to electrophoresis and the DPP4 and actin proteins visualized by Western blotting. (C) 293 cells were transfected with HuDPP4 (1 μg) in conjunction with the indicated TMPRSS2 doses. After 1 day, the HuDPP4, TMPR, and actin proteins in cell lysates were visualized by Western blotting. The uncleaved (inactive) TMPRSS2 zymogen has a molecular mass of ~60 kDa, and proteolytically active (WT) TMPRSS2 has a molecular mass of ~25 kDa.

SARS-CoV receptor, angiotensin converting enzyme 2 (21), and augments SARS pseudovirus entry (37), we further investigated DPP4 proteolysis at higher TMPRSS2 levels and in human 293 cells. In these experiments, human DPP4 levels clearly diminished with increasing TMPRSS2 levels, in similarity to the results seen with the receptor for SARS-CoV, but only at supraphysiological TMPRSS2 levels (Fig. 7C). In sum, the main conclusion from these studies involving TMPRSS2, one of the principal MERS-CoV-activating proteases, is that cells bearing receptors with low affinities for MERS-CoV are rendered far more susceptible to infection when the appropriate proteolytic environments are in place.

DISCUSSION

MERS-CoV preferentially infected cells expressing human DPP4, and its S1 domain bound to human DPP4 with higher affinity than to any of the other orthologous animal DPP4s. Thus, it is possible that the MERS-CoVs (2012 and 2013 isolates), even with their limited residence in human hosts, are modestly "human adapted." We suggest that the proximal source of the human-adapted MERS-CoV includes animals whose DPP4 proteins bind to MERS-CoV at near-human levels of DPP4 affinity. These animals are likely to maintain a MERS-CoV population that includes variants with relatively high affinities for human receptors that thus become the founders that intrude into the human population. Our results suggest that camels and horses can harbor these human founder viruses. Goats and bats may be less prominent hosts for "human" MERS-CoVs, as their DPP4s are less adherent to the human MERS-CoV. However, a very recent report documenting the susceptibility of two goat cell lines to MERS-CoV (38) makes it clear that goats cannot be excluded from the roster of animals potentially transmitting the virus to humans. Definitive exclusion from the MERS-CoV transmission processes applies to mice and also to ferrets, as a recent publication demonstrated that ferret DPP4 did not bind MERS S1 or support MERS-CoV infection (39). Quite likely, there are several mammals entirely refractory to MERS-CoV binding and thus resistant to infection.

The affinity of the MERS-CoV S RBD for human DPP4 is ~17 nM (26). This value is ~10 times lower than that of the SARS-CoV S RBD for human ACE2 (40). These findings suggest that the MERS-CoV could further adapt to the human DPP4, in the same ways that SARS-CoV adapted to humans. Indeed, the presumed animal precursors of human SARS-CoVs have affinities for ACE2 in the ~20 to ~100 nM range (40), and the higher ~2 nM affinities of human-adapted SARS-CoV are considered to be central contributors to epidemic potential (41, 42). Thus, careful monitoring of human and animal MERS-like CoV spike RBD changes is critical for assessing the likelihood of epidemic spread.

It is notable, however, that there appears to be limited diversity in human MERS-CoVs. Nearly identical MERS-CoVs have appar-

ently transmitted from animal to human on more than one occasion and in more than one geographic location (15). This observation is most consistent with the notion that a single animal species, harboring MERS-CoV populations of restricted genomic diversity, served as the reservoir for all human transmission thus far. Furthermore, once in humans, while there is evidence of some genetic drift, there are no changes in the MERS-CoV spike RBDs (15). Even in virus isolates from patients with comorbidities that impaired antiviral immune responses, and in whom virus might be expected to persist, there is no evidence for changes in the MERS-CoV S RBD. While this apparent genetic stability may simply reflect the small number of human infections and the limited analysis of virus isolates, it is also possible that there is little selective force for change at the level of virus-receptor binding.

A genetically stable MERS-CoV RBD suggests that binding affinity to the DPP4 receptor may not be the most critical factor for adaptation to new species. MERS-CoV may have stably adapted to an affinity range (~10 to ~20 nM) that allows relatively similar levels of strength of binding to many different animal DPP4s, i.e., human, camel, and horse, and consequent facile transfer between species. This affinity range, however, makes MERS-CoV considerably less adherent than human SARS-CoV for its human ACE2 receptors. It is possible that affinity requirements relate to virus entry events following receptor binding. For SARS-CoV, endocytosis typically precedes S protein proteolysis and tethering of virus to cells via S protein fusion machinery (43, 44). A durable virus-receptor connection may therefore be necessary to maintain SARS-CoV on cells throughout endocytosis or at least until its S proteins refold into "fusion-intermediate" forms that directly connect the viral and cellular membranes in a receptor-independent fashion. In contrast, MERS-CoV appears to more rapidly adopt the fusion-intermediate, membrane-tethering forms at the target cell plasma membrane and thus may not require such long-lasting association with receptors. This notion is supported by the fact that, unlike SARS-CoV (45), MERS-CoV infection is quite sensitive to a membrane-impermeant inhibitory peptide that targets the fusion intermediate forms (46). Additionally, MERS-CoV infection is remarkably increased by TMPRSS2, a cell surface protease that quite likely cleaves and exposes S protein fusion machinery immediately after receptor binding (19). Our results show that the weakly adhesive goat and bat DPP4s were especially assisted by TMPRSS2 (Fig. 7A and B), suggesting that a low-affinity receptor can sensitize cells to infection as long as there are protease cofactors available to cleave viral spikes and permit their transitions into membrane fusion-active conformations.

While no MERS-CoV RBD mutations have been detected, adaptations in its membrane fusion machinery have been repeatedly observed (15, 30). With the caveat that the data on MERS-CoV diversity are quite limited, we suggest that the selective forces in MERS-CoV are at the level beyond RBD interaction and that the MERS-CoV has adapted to a more immediate cell surface proteolysis which does not demand this sort of stable association with receptors. Indeed, high-affinity receptor interaction may not be a requisite feature of all CoV infections. More relevant to infection may be the host cell proteases and the fusion activation process. These views are consistent with previous hypotheses proposing that enveloped virus-receptor affinities adapt to the minimum levels sufficient to allow for the next membrane fusion stage (34).

ACKNOWLEDGMENTS

This work was supported by a grant from the National Institutes of Health (AI-P01 060699; S.P., P.B.M., and T.G.) and by the Roy J. Carver Charitable Trust (P.B.M.).

REFERENCES

1. **The WHO MERS-CoV Research Group.** 12 November 2013. State of knowledge and data gaps of Middle East respiratory syndrome coronavirus (MERS-CoV) in humans. PLoS Curr. http://dx.doi.org/10.1371/currents.outbreaks.0bf719e352e7478f8ad85fa30127ddb8.
2. **Assiri A, Al-Tawfiq JA, Al-Rabeeah AA, Al-Rabiah FA, Al-Hajjar S, Al-Barrak A, Flemban H, Al-Nassir WN, Balkhy HH, Al-Hakeem RF, Makhdoom HQ, Zumla AI, Memish ZA.** 2013. Epidemiological, demographic, and clinical characteristics of 47 cases of Middle East respiratory syndrome coronavirus disease from Saudi Arabia: a descriptive study. Lancet Infect. Dis. **13:**752–761. http://dx.doi.org/10.1016/S1473-3099(13)70204-4.
3. **Guery B, Poissy J, el Mansouf L, Sejourne C, Ettahar N, Lemaire X, Vuotto F, Goffard A, Behillil S, Enouf V, Caro V, Mailles A, Che D, Manuguerra JC, Mathieu D, Fontanet A, van der Werf S.** 2013. Clinical features and viral diagnosis of two cases of infection with Middle East respiratory syndrome coronavirus: a report of nosocomial transmission. Lancet **381:**2265–2272. http://dx.doi.org/10.1016/S0140-6736(13)60982-4.
4. **Lim PL, Lee TH, Rowe EK.** 2013. Middle East respiratory syndrome coronavirus (MERS CoV): update 2013. Curr. Infect. Dis. Rep. **15:**295–298. http://dx.doi.org/10.1007/s11908-013-0344-2.
5. **Centers for Disease Control and Prevention (CDC).** 2013. Updated information on the epidemiology of Middle East respiratory syndrome coronavirus (MERS-CoV) infection and guidance for the public, clinicians, and public health authorities, 2012–2013. MMWR Morb Mortal. Wkly. Rep. **62:**793–796.
6. **Falzarano D, de Wit E, Martellaro C, Callison J, Munster VJ, Feldmann H.** 2013. Inhibition of novel beta coronavirus replication by a combination of interferon-alpha2b and ribavirin. Sci. Rep. **3:**1686. http://dx.doi.org/10.1038/srep01686.
7. **Falzarano D, de Wit E, Rasmussen AL, Feldmann F, Okumura A, Scott DP, Brining D, Bushmaker T, Martellaro C, Baseler L, Benecke AG, Katze MG, Munster VJ, Feldmann H.** 2013. Treatment with interferon-alpha2b and ribavirin improves outcome in MERS-CoV-infected rhesus macaques. Nat. Med. **19:**1313–1317. http://dx.doi.org/10.1038/nm.3362.
8. **Memish ZA, Mishra N, Olival KJ, Fagbo SF, Kapoor V, Epstein JH, Alhakeem R, Durosinloun A, Al Asmari M, Islam A, Kapoor A, Briese T, Daszak P, Al Rabeeah AA, Lipkin WI.** 2013. Middle East respiratory syndrome coronavirus in bats, Saudi Arabia. Emerg. Infect. Dis. **19:**1819–1823. http://dx.doi.org/10.3201/eid1911.131172.
9. **Ithete NL, Stoffberg S, Corman VM, Cottontail VM, Richards LR, Schoeman MC, Drosten C, Drexler JF, Preiser W.** 2013. Close relative of human middle East respiratory syndrome coronavirus in bat, South Africa. Emerg. Infect. Dis. **19:**1697–1699. http://dx.doi.org/10.3201/eid1910.130946.
10. **Lau SK, Li KS, Tsang AK, Lam CS, Ahmed S, Chen H, Chan KH, Woo PC, Yuen KY.** 2013. Genetic characterization of Betacoronavirus lineage C viruses in bats reveals marked sequence divergence in the spike protein of pipistrellus bat coronavirus HKU5 in Japanese pipistrelle: implications for the origin of the novel Middle East respiratory syndrome coronavirus. J. Virol. **87:**8638–8650. http://dx.doi.org/10.1128/JVI.01055-13.
11. **Ge XY, Li JL, Yang XL, Chmura AA, Zhu G, Epstein JH, Mazet JK, Hu B, Zhang W, Peng C, Zhang YJ, Luo CM, Tan B, Wang N, Zhu Y, Crameri G, Zhang SY, Wang LF, Daszak P, Shi ZL.** 2013. Isolation and characterization of a bat SARS-like coronavirus that uses the ACE2 receptor. Nature **503:**535–538. http://dx.doi.org/10.1038/nature12711.
12. **Reusken CB, Haagmans BL, Muller MA, Gutierrez C, Godeke GJ, Meyer B, Muth D, Raj VS, Vries LS, Corman VM, Drexler JF, Smits SL, El Tahir YE, De Sousa R, van Beek J, Nowotny N, van Maanen K, Hidalgo-Hermoso E, Bosch BJ, Rottier P, Osterhaus A, Gortazar-Schmidt C, Drosten C, Koopmans MP.** 2013. Middle East respiratory syndrome coronavirus neutralising serum antibodies in dromedary camels: a comparative serological study. Lancet Infect. Dis. **13:**859–866. http://dx.doi.org/10.1016/S1473-3099(13)70164-6.
13. **Perera R, Wang P, Gomaa M, El-Shesheny R, Kandeil A, Bagato O, Siu L, Shehata M, Kayed A, Moatasim Y, Li M, Poon L, Guan Y, Webby R, Ali M, Peiris J, Kayali G.** 2013. Seroepidemiology for MERS coronavirus using microneutralisation and pseudoparticle virus neutralisation assays reveal a high prevalence of antibody in dromedary camels in Egypt, June

2013. Euro Surveill. **18**(**36**):pii=20574. http://www.eurosurveillance.org/ViewArticle.aspx?ArticleId=20574.
14. **Haagmans BL, Al Dhahiry SH, Reusken CB, Raj VS, Galiano M, Myers R, Godeke GJ, Jonges M, Farag E, Diab A, Ghobashy H, Alhajri F, Al-Thani M, Al-Marri SA, Al Romaihi HE, Al Khal A, Bermingham A, Osterhaus AD, Alhajri MM, Koopmans MP.** 2014. Middle East respiratory syndrome coronavirus in dromedary camels: an outbreak investigation. Lancet Infect. Dis. **14:**140–145. http://dx.doi.org/10.1016/S1473-3099(13)70690-X.
15. **Cotten M, Watson SJ, Kellam P, Al-Rabeeah AA, Makhdoom HQ, Assiri A, Al-Tawfiq JA, Alhakeem RF, Madani H, Alrabiah FA, Hajjar SA, Al-Nassir WN, Albarrak A, Flemban H, Balkhy HH, Alsubaie S, Palser AL, Gall A, Bashford-Rogers R, Rambaut A, Zumla AI, Memish ZA.** 2013. Transmission and evolution of the Middle East respiratory syndrome coronavirus in Saudi Arabia: a descriptive genomic study. Lancet **382:**1993–2002. http://dx.doi.org/10.1016/S0140-6736(13)61887-5.
16. **Breban R, Riou J, Fontanet A.** 2013. Interhuman transmissibility of Middle East respiratory syndrome coronavirus: estimation of pandemic risk. Lancet **382:**694–699. http://dx.doi.org/10.1016/S0140-6736(13)61492-0.
17. **Raj VS, Mou H, Smits SL, Dekkers DH, Muller MA, Dijkman R, Muth D, Demmers JA, Zaki A, Fouchier RA, Thiel V, Drosten C, Rottier PJ, Osterhaus AD, Bosch BJ, Haagmans BL.** 2013. Dipeptidyl peptidase 4 is a functional receptor for the emerging human coronavirus-EMC. Nature **495:**251–254. http://dx.doi.org/10.1038/nature12005.
18. **Gierer S, Bertram S, Kaup F, Wrensch F, Heurich A, Kramer-Kuhl A, Welsch K, Winkler M, Meyer B, Drosten C, Dittmer U, von Hahn T, Simmons G, Hofmann H, Pohlmann S.** 2013. The spike protein of the emerging betacoronavirus EMC uses a novel coronavirus receptor for entry, can be activated by TMPRSS2, and is targeted by neutralizing antibodies. J. Virol. **87:**5502–5511. http://dx.doi.org/10.1128/JVI.00128-13.
19. **Shirato K, Kawase M, Matsuyama S.** 2013. Middle East respiratory syndrome coronavirus (MERS-CoV) infection mediated by the transmembrane serine protease TMPRSS2. J. Virol. **87:**12552–12561. http://dx.doi.org/10.1128/JVI.01890-13.
20. **Gibson DG, Young L, Chuang RY, Venter JC, Hutchison CA, III, Smith HO.** 2009. Enzymatic assembly of DNA molecules up to several hundred kilobases. Nat. Methods **6:**343–345. http://dx.doi.org/10.1038/nmeth.1318.
21. **Shulla A, Heald-Sargent T, Subramanya G, Zhao J, Perlman S, Gallagher T.** 2011. A transmembrane serine protease is linked to the severe acute respiratory syndrome coronavirus receptor and activates virus entry. J. Virol. **85:**873–882. http://dx.doi.org/10.1128/JVI.02062-10.
22. **Whitt MA.** 2010. Generation of VSV pseudotypes using recombinant DeltaG-VSV for studies on virus entry, identification of entry inhibitors, and immune responses to vaccines. J. Virol. Methods **169:**365–374. http://dx.doi.org/10.1016/j.jviromet.2010.08.006.
23. **Gallagher TM.** 1997. A role for naturally occurring variation of the murine coronavirus spike protein in stabilizing association with the cellular receptor. J. Virol. **71:**3129–3137.
24. **Engel M, Hoffmann T, Wagner L, Wermann M, Heiser U, Kiefersauer R, Huber R, Bode W, Demuth HU, Brandstetter H.** 2003. The crystal structure of dipeptidyl peptidase IV (CD26) reveals its functional regulation and enzymatic mechanism. Proc. Natl. Acad. Sci. U. S. A. **100:**5063–5068. http://dx.doi.org/10.1073/pnas.0230620100.
25. **Chen Y, Rajashankar KR, Yang Y, Agnihothram SS, Liu C, Lin YL, Baric RS, Li F.** 2013. Crystal structure of the receptor-binding domain from newly emerged Middle East respiratory syndrome coronavirus. J. Virol. **87:**10777–10783. http://dx.doi.org/10.1128/JVI.01756-13.
26. **Lu G, Hu Y, Wang Q, Qi J, Gao F, Li Y, Zhang Y, Zhang W, Yuan Y, Bao J, Zhang B, Shi Y, Yan J, Gao GF.** 2013. Molecular basis of binding between novel human coronavirus MERS-CoV and its receptor CD26. Nature **500:**227–231. http://dx.doi.org/10.1038/nature12328.
27. **Wang N, Shi X, Jiang L, Zhang S, Wang D, Tong P, Guo D, Fu L, Cui Y, Liu X, Arledge KC, Chen YH, Zhang L, Wang X.** 2013. Structure of MERS-CoV spike receptor-binding domain complexed with human receptor DPP4. Cell Res. **23:**986–993. http://dx.doi.org/10.1038/cr.2013.92.
28. **Weihofen WA, Liu J, Reutter W, Saenger W, Fan H.** 2004. Crystal structure of CD26/dipeptidyl-peptidase IV in complex with adenosine deaminase reveals a highly amphiphilic interface. J. Biol. Chem. **279:**43330–43335. http://dx.doi.org/10.1074/jbc.M405001200.
29. **Kameoka J, Tanaka T, Nojima Y, Schlossman SF, Morimoto C.** 1993. Direct association of adenosine deaminase with a T cell activation antigen, CD26. Science **261:**466–469. http://dx.doi.org/10.1126/science.8101391.
30. **Scobey T, Yount BL, Sims AC, Donaldson EF, Agnihothram SS, Menachery VD, Graham RL, Swanstrom J, Bove PF, Kim JD, Grego S, Randell SH, Baric RS.** 2013. Reverse genetics with a full-length infectious cDNA of the Middle East respiratory syndrome coronavirus. Proc. Natl. Acad. Sci. U. S. A. **110:**16157–16162. http://dx.doi.org/10.1073/pnas.1311542110.
31. **Coleman CM, Matthews KL, Goicochea L, Frieman MB.** 2014. Wild type and innate immune deficient mice are not susceptible to the Middle East respiratory syndrome coronavirus. J. Gen. Virol. **95**(Pt 2):408–412. http://dx.doi.org/10.1099/vir.0.060640-0.
32. **Du L, Zhao G, Kou Z, Ma C, Sun S, Poon VK, Lu L, Wang L, Debnath AK, Zheng BJ, Zhou Y, Jiang S.** 2013. Identification of a receptor-binding domain in the s protein of the novel human coronavirus Middle East respiratory syndrome coronavirus as an essential target for vaccine development. J. Virol. **87:**9939–9942. http://dx.doi.org/10.1128/JVI.01048-13.
33. **Mou H, Raj VS, van Kuppeveld FJ, Rottier PJ, Haagmans BL, Bosch BJ.** 2013. The receptor binding domain of the new Middle East respiratory syndrome coronavirus maps to a 231-residue region in the spike protein that efficiently elicits neutralizing antibodies. J. Virol. **87:**9379–9383. http://dx.doi.org/10.1128/JVI.01277-13.
34. **Hasegawa K, Hu C, Nakamura T, Marks JD, Russell SJ, Peng KW.** 2007. Affinity thresholds for membrane fusion triggering by viral glycoproteins. J. Virol. **81:**13149–13157. http://dx.doi.org/10.1128/JVI.01415-07.
35. **Simmons G, Zmora P, Gierer S, Heurich A, Pohlmann S.** 2013. Proteolytic activation of the SARS-coronavirus spike protein: cutting enzymes at the cutting edge of antiviral research. Antiviral Res. **100:**605–614. http://dx.doi.org/10.1016/j.antiviral.2013.09.028.
36. **Hooper JD, Clements JA, Quigley JP, Antalis TM.** 2001. Type II transmembrane serine proteases. Insights into an emerging class of cell surface proteolytic enzymes. J. Biol. Chem. **276:**857–860. http://dx.doi.org/10.1074/jbc.R000020200.
37. **Heurich A, Hofmann-Winkler H, Gierer S, Liepold T, Jahn O, Pohlmann S.** 2014. TMPRSS2 and ADAM17 cleave ACE2 differentially and only proteolysis by TMPRSS2 augments entry driven by the severe acute respiratory syndrome coronavirus spike protein. J. Virol. **88:**1293–1307. http://dx.doi.org/10.1128/JVI.02202-13.
38. **Eckerle I, Corman VM, Muller MA, Lenk M, Ulrich RG, Drosten C.** 2014. Replicative capacity of MERS coronavirus in livestock cell lines. Emerg. Infect. Dis. **20:**276–279. http://dx.doi.org/10.3201/eid2002.131182.
39. **Raj VS, Smits SL, Provacia LB, van den Brand JM, Wiersma L, Ouwendijk WJ, Bestebroer TM, Spronken MI, van Amerongen G, Rottier PJ, Fouchier RA, Bosch BJ, Osterhaus AD, Haagmans BL.** 2014. Adenosine deaminase acts as a natural antagonist for dipeptidyl peptidase 4-mediated entry of the Middle East respiratory syndrome coronavirus. J. Virol. **88:**1834–1838. http://dx.doi.org/10.1128/JVI.02935-13.
40. **Wu K, Peng G, Wilken M, Geraghty RJ, Li F.** 2012. Mechanisms of host receptor adaptation by severe acute respiratory syndrome coronavirus. J. Biol. Chem. **287:**8904–8911. http://dx.doi.org/10.1074/jbc.M111.325803.
41. **Li W, Zhang C, Sui J, Kuhn JH, Moore MJ, Luo S, Wong SK, Huang IC, Xu K, Vasilieva N, Murakami A, He Y, Marasco WA, Guan Y, Choe H, Farzan M.** 2005. Receptor and viral determinants of SARS-coronavirus adaptation to human ACE2. EMBO J. **24:**1634–1643. http://dx.doi.org/10.1038/sj.emboj.7600640.
42. **Li W, Wong SK, Li F, Kuhn JH, Huang IC, Choe H, Farzan M.** 2006. Animal origins of the severe acute respiratory syndrome coronavirus: insight from ACE2-S-protein interactions. J. Virol. **80:**4211–4219. http://dx.doi.org/10.1128/JVI.80.9.4211-4219.2006.
43. **Wang H, Yang P, Liu K, Guo F, Zhang Y, Zhang G, Jiang C.** 2008. SARS coronavirus entry into host cells through a novel clathrin- and caveolae-independent endocytic pathway. Cell Res. **18:**290–301. http://dx.doi.org/10.1038/cr.2008.15.
44. **Simmons G, Gosalia DN, Rennekamp AJ, Reeves JD, Diamond SL, Bates P.** 2005. Inhibitors of cathepsin L prevent severe acute respiratory syndrome coronavirus entry. Proc. Natl. Acad. Sci. U. S. A. **102:**11876–11881. http://dx.doi.org/10.1073/pnas.0505577102.
45. **Bosch BJ, Martina BE, Van Der Zee R, Lepault J, Haijema BJ, Versluis C, Heck AJ, De Groot R, Osterhaus AD, Rottier PJ.** 2004. Severe acute respiratory syndrome coronavirus (SARS-CoV) infection inhibition using spike protein heptad repeat-derived peptides. Proc. Natl. Acad. Sci. U. S. A. **101:**8455–8460. http://dx.doi.org/10.1073/pnas.0400576101.
46. **Gao J, Lu G, Qi J, Li Y, Wu Y, Deng Y, Geng H, Li H, Wang Q, Xiao H, Tan W, Yan J, Gao GF.** 2013. Structure of the fusion core and inhibition of fusion by a heptad-repeat peptide derived from the S protein of MERS-CoV. J. Virol. **87:**13134–13140. http://dx.doi.org/10.1128/JVI.02433-13.